

LEGIBILITY NOTICE

A major purpose of the Technical Information Center is to provide the broadest dissemination possible of information contained in DOE's Research and Development Reports to business, industry, the academic community, and federal, state and local governments.

Although a small portion of this report is not reproducible, it is being made available to expedite the availability of information on the research discussed herein.

CONF-9010156--1

Los Alamos National Laboratory is operated by the University of California for the United States Department of Energy under contract W-7405-ENG-36

LA-UR--90-2552

DE90 015056

TITLE SPATIAL LOCALIZATION OF NEURAL SOURCES USING THE MAGNETOENCEPHALOGRAPH

AUTHOR(S) John C. Mosher, Paul S. Lewis, and Richard Leahy

SUBMITTED TO Fifth ASSP Workshop on Spectrum Estimation and Modeling, Rochester, NY, October 10-12, 1990

DISCLAIMER


This report was prepared as an account of work sponsored by an agency of the United States Government. Neither the United States Government nor any agency thereof, nor any of their employees, makes any warranty, express or implied, or assumes any legal liability or responsibility for the accuracy, completeness, or usefulness of any information, apparatus, product, or process disclosed, or represents that its use would not infringe privately owned rights. Reference herein to any specific commercial product, process, or service by trade name, trademark, manufacturer, or otherwise does not necessarily constitute or imply its endorsement, recommendation, or favoring by the United States Government or any agency thereof. The views and opinions of authors expressed herein do not necessarily state or reflect those of the United States Government or any agency thereof.

By acceptance of this article, the publisher recognizes that the U.S. Government retains a nonexclusive, royalty-free license to publish or reproduce the published form of this contribution, or to allow others to do so, for U.S. Government purposes.

The Los Alamos National Laboratory requests that the publisher identify this article as work performed under the auspices of the U.S. Department of Energy.

Los Alamos Los Alamos National Laboratory
Los Alamos, New Mexico 87545

FORM NO. 100-100
100-100-100-100

MASTER 
DISTRIBUTION OF THIS DOCUMENT IS UNLIMITED

SPATIAL LOCALIZATION OF NEURAL SOURCES USING THE MAGNETOENCEPHALOGRAM*

John C. Mosher^{†‡}, Paul S. Lewis*, and Richard Leahy[†]

[†]Signal and Image Processing Institute, Department of Electrical Engineering-Systems,
University of Southern California MC 0272, Los Angeles, California 90089-0272

*Los Alamos National Laboratory, Mechanical & Electronic Engineering,
MEE-3, MS J580, Los Alamos, New Mexico 87545

[‡]TRW Systems Engineering & Development Division,
DH4-2139 One Space Park, Redondo Beach, California 90278

ABSTRACT

An array of Superconducting QUantum Interference Device (SQUID) biomagnetometers may be used to measure the spatio-temporal neuromagnetic field or magnetoencephalogram (MEG) produced by the brain in response to a given sensory stimulus. A popular model for the neural activity that produces these fields is a set of current dipoles. We assume that the location, orientation, and magnitude of the dipoles are unknown. We show how the problem may be decomposed into the estimation of the dipole locations using nonlinear minimization followed by linear estimation of the associated moment time series. The methods described are demonstrated in a simulated application to a three dipole problem. Cramer-Rao lower bounds are derived for the white Gaussian noise case.

1 Introduction

The recent development of the SQUID biomagnetometer has made it possible to detect and acquire measurements of the very weak magnetic fields produced by neural activity within the human brain. Using an array of SQUID biomagnetometers, we can simultaneously acquire time-series measurements of the transient neuromagnetic field at a number of different sites. To deduce neural activity patterns from these measurements requires solving an inverse problem—computing the neural current sources from the magnetic fields that they produce. Physically, this inverse problem is under-determined, so *a priori* modeling assumptions must be made about the underlying neural current distributions in order to reach any “solution” (see [1] for an overview). The simplest and most widely used composite model is the “dipole in a sphere.” Here, the impressed current is modeled as a current dipole, and the head is modeled as a uniformly conductive sphere.

Most MEG research involves a transient evoked response, which is neural activity occurring in response to

some sensory input, typically an auditory or visual stimulus. A current dipole can accurately model neural activity localized to one site, representing the coherent activation of hundreds of individual neurons [2]. With this model, the inverse problem reduces to the nonlinear optimization problem of computing the location and moment parameters of the dipole whose field best matches the measurements in a least-squares sense. For more complex or distributed evoked responses, the model can be extended to include multiple dipoles. As in all modeling situations, a trade-off exists between model complexity and generality and the ability to estimate reliably the model parameters from the given measurement data. To increase the complexity of the source spatial models that can be effectively employed, MEG researchers have begun to incorporate temporal modeling assumptions. The addition of a temporal model increases the range of the measurements that can be used in model fitting from the spatial to the temporal domain.

A spatio-temporal dipole model and the necessary associated assumptions are presented in [2]. MEG researchers differ in how they describe the time variation of the data. In [3], details of these models and their similarity in formulation are described. In this paper, we restrict ourselves to the “rotating” dipole model and present Cramer-Rao lower bounds for the white Gaussian noise case.

2 Data Models

In this section, we present the Biot-Savart law in a convenient discrete matrix notation, which we then use to develop a spatio-temporal dipole model commonly used in MEG research. The general model is $\mathbf{B} = \mathbf{G}(\theta)\mathbf{T}$, where the set $\{\theta, \mathbf{T}\}$ contains our unknown parameters. The parameters \mathbf{T} can always be found using a direct pseudoinverse solution, but in general the parameters in θ must be found using an iterative nonlinear minimization algorithm [3].

2.1 Biot-Savart Law

The inverse problem considered here is one of taking many measurements of the magnetic vector field at discrete lo-

*This work was supported in part by the TRW Doctoral Fellowship Program; Los Alamos National Laboratory, operated by the University of California for the United States Department of Energy under contract W-7405-ENG-36; and by the Z. A. Kaprielian Innovative Research Fund at the University of Southern California.

cations about the head and attempting to determine the underlying current source distribution. We begin by examining the model for a single dipole, then expand this model to account for multiple dipoles.

Establishing an origin, denoting the dipole position as \vec{L} , and observing the i th measurement at receiver location $\vec{R}(i)$, the Biot-Savart law for a current dipole can be written as

$$\vec{B}(i) = k \frac{\vec{M} \times (\vec{R}(i) - \vec{L})}{|\vec{R}(i) - \vec{L}|^3} \quad (1)$$

where,

- k : constant $\mu_0/(4\pi)$
- \vec{M} : dipole moment (gain and orientation)
- \vec{L} : dipole location
- $\vec{R}(i)$: i th measurement receiver location
- $\vec{B}(i)$: full magnetic field at $\vec{R}(i)$

A SQUID biomagnetometer is used to acquire the magnetic field at position $\vec{R}(i)$, but only measures one component of the three-dimensional field. Thus only a scalar measurement is made:

$$B(i) = \vec{B}(i) \cdot \hat{s}(i) \quad (2)$$

where $\hat{s}(i)$ denotes the unit orientation of the i th sensor and hence the component of the magnetic field acquired, and the operation " \cdot " denotes the inner product of two vectors. Combining equations (1) and (2) and manipulating the resulting triple scalar product yields

$$B(i) = k \frac{(\vec{R}(i) - \vec{L}) \times \hat{s}(i) \cdot \vec{M}}{|\vec{R}(i) - \vec{L}|^3} = \vec{g}(i) \cdot \vec{M} \quad (3)$$

The vector $\vec{g}(i)$ can be viewed as a gain vector, relating the moment intensity of the dipole to the measurement at position $\vec{R}(i)$. If we let each gain vector be represented as a 1×3 row vector and the moment as a 3×1 column vector, then we can arrange the measurements from m spatially distributed receivers in a matrix form,

$$\mathbf{B} = \begin{bmatrix} B(1) \\ \vdots \\ B(m) \end{bmatrix} = \begin{bmatrix} \vec{g}(1) \\ \vdots \\ \vec{g}(m) \end{bmatrix} [\vec{M}] = \mathbf{G}(\theta) \mathbf{T} \quad (4)$$

The parameters in θ represent the unknown position \vec{L} , and \mathbf{T} represents the unknown moment orientation \vec{M} . The matrix $\mathbf{G}(\theta)$ can be considered the gain or relationship between a unit moment source at \vec{L} and the column vector of receiver locations $\{\vec{R}(i)\}$. From this form we clearly see the linear relationship between the moment and the measurements. This model easily extends to the multiple dipole case by superposition. For p dipoles,

$$\mathbf{B} = [\mathbf{G}_1, \dots, \mathbf{G}_p] \begin{bmatrix} \mathbf{T}_1 \\ \vdots \\ \mathbf{T}_p \end{bmatrix} \quad (5)$$

or simply $\mathbf{B} = \mathbf{G} \mathbf{T}$, where \mathbf{G} can be partitioned into the smaller matrices \mathbf{G}_p (as defined in (4)); similarly \mathbf{T} may be partitioned as the concatenation of the moment vectors for each of the p dipoles. Thus for m sensors and p dipoles, \mathbf{B} is $m \times 1$, matrix \mathbf{G} is $m \times 3p$, and vector \mathbf{T} is $3p \times 1$.

For simplicity in deriving the model, the biomagnetometer is assumed to make a perfect point field measurement. However, the finite coil area and gradiometer configuration of a practical SQUID biomagnetometer, as well as other effects such as head and source models, can also be included into the model, resulting in a very similar formulation to that presented here [4].

The above expression is for a single time slice of data, but evoked response data are usually collected as samples over a segment of time. The result is a spatio-temporal data matrix $\mathbf{B} = [\mathbf{B}(1), \dots, \mathbf{B}(N)]$ of m spatial measurements by N temporal measurements. MEG researchers differ in the constraints that should be placed on the location and moment parameters. In [3], the different constrained models are reviewed. In this paper the model restricts the location of the dipoles to be constant throughout the measurement interval, but allows the moment intensities and orientations to vary. The data matrix is then formed as

$$\mathbf{B} = \mathbf{G}(\theta) [\mathbf{T}(1), \dots, \mathbf{T}(N)] = \mathbf{G}(\theta) \mathbf{T} \quad (6)$$

Each column of the \mathbf{T} matrix may be partitioned to represent the moments of p dipoles at time j ,

$$\mathbf{T}(j) = \begin{bmatrix} \vec{M}_1(j) \\ \vdots \\ \vec{M}_p(j) \end{bmatrix} \quad (7)$$

and each partition $\vec{M}_i(j)$ itself can be represented by its *dipole source components* [5]. Hence each row of \mathbf{T} represents the time series for one component of one dipole. Since no constraints are placed on the time series of the three components for each dipole, the orientation of the dipole can vary or "rotate" over time.

3 Error Bounds

This model assumes that the location, orientation, and magnitude of the dipoles are unknown. We measure a set of data \mathbf{F} , which we model as $\mathbf{F} = \mathbf{G}(\theta) \mathbf{T} + \mathbf{N}$, where \mathbf{N} is the unknown noise, and we set our measure of fit to be the least-squares fit between model and data. If the noise in each sample is i.i.d. zero-mean Gaussian, then the parameters that minimize this squared error are the maximum likelihood estimate of \mathbf{F} .

We can approach this problem as belonging to the class of nonlinear least squares problems whose variables separate [6]. This approach focuses the inverse problem to that of solving for the parameters in the matrix \mathbf{G} , since the parameters in \mathbf{T} can be replaced with their least squares or minimum norm solution. This approach is well known in the array processing community, (e.g., [7]), and in [3].

we presented the specific details for the MEG problem. In this paper, we wish to focus our efforts on bounding the error of such an estimator.

3.1 The Cramer-Rao Bound

In this subsection, we will adapt our notation to effectively use the results of Stoica [7] for most of the proof; however, unlike Stoica, we restrict ourselves to real data while expanding our definition of his array manifold.

We assume that the unknown parameters are the variance of the noise, σ^2 , the moment time series, $\mathbf{I}(j)$, and the dipole locations in θ . For convenience, we will group these parameters into one vector ψ ,

$$\psi = [\sigma^2, \mathbf{I}(1)^T, \dots, \mathbf{I}(N)^T, \bar{L}_1, \dots, \bar{L}_p]^T \quad (8)$$

where we have now explicitly listed the location parameters in θ for the p dipoles. We also recall that $\mathbf{G}(\theta)$ has the partitioned structure $\mathbf{G} = [\mathbf{G}_1, \dots, \mathbf{G}_p]$, where each partition is itself $m \times 3$; similarly, $\mathbf{I}(j)$ can also be partitioned as the concatenation of the moment vectors for each of the p dipoles, $\mathbf{I}(j)^T = [\mathbf{I}_1(j)^T, \dots, \mathbf{I}_p(j)^T]$.

Theorem 1 (Cramer-Rao Inequality) *For the set of data \mathbf{F} and the stated probability distribution function of the noise, let $\hat{\psi}$ be any unbiased estimate of the deterministic parameters based on $\mathbf{F} = \mathbf{G}(\theta)\mathbf{T} + \mathbf{N}$. Then*

$$\mathbf{E}\{(\psi - \hat{\psi})(\psi - \hat{\psi})^T\} \geq \mathbf{J}^{-1} \quad (9)$$

where \mathbf{J} is the Fisher information matrix,

$$\mathbf{J} = \mathbf{E}\left\{\left[\frac{\delta}{\delta\psi} \ln p(\mathbf{N})\right] \left[\frac{\delta}{\delta\psi} \ln p(\mathbf{N})\right]^T\right\} \quad (10)$$

Proof: See for example [8]. To calculate the Fisher information matrix, we need to calculate partial derivatives of the log-likelihood function and then take expected values of the outer product. For the case of spatially and temporally white Gaussian noise with variance σ^2 , the log-likelihood function is straightforward to calculate for m sensors and N time samples, yielding

$$\begin{aligned} \ln l = & -Nm \ln(\sqrt{2\pi}) - \frac{1}{2} Nm \ln(\sigma^2) \\ & - \frac{1}{2\sigma^2} \sum_{j=1}^N \|\mathbf{E}(j) - \mathbf{G}(\theta)\mathbf{T}(j)\|^2. \end{aligned} \quad (11)$$

The partials with respect to variance and moments are straightforward to calculate, as in [7],

$$\frac{\delta \ln l}{\delta(\sigma^2)} = -\frac{Nm}{2\sigma^2} + \frac{1}{2\sigma^4} \sum_{j=1}^N \mathbf{E}(j)^T \mathbf{E}(j) \quad (12)$$

and

$$\frac{\delta \ln l}{\delta \mathbf{T}(j)} = \frac{1}{\sigma^2} \mathbf{G}^T \mathbf{E}(j), \quad j = 1, \dots, N \quad (13)$$

The partials with respect to the locations requires careful attention to notation, which deviates somewhat from

that of Stoica due to the expanded form of the matrix \mathbf{G} . Each of the p dipole locations \bar{L}_k is itself represented by three parameters, which we will here denote by Cartesian coordinates L_{xk} , L_{yk} , and L_{zk} . Consider the partial with respect to L_{xk} ,

$$\frac{\delta \ln l}{\delta L_{xk}} = \frac{1}{\sigma^2} \sum_{j=1}^N \left[\frac{\delta \mathbf{G}}{\delta L_{xk}} \mathbf{T}(j) \right]^T \mathbf{E}(j) \quad (14)$$

which in turn requires the partial of the gain matrix. Now consider that only the k th partition of the gain matrix is a function of location L_{xk} ,

$$\frac{\delta \mathbf{G}}{\delta L_{xk}} = [0, \dots, 0, \frac{\delta \mathbf{G}_k}{\delta L_{xk}}, 0, \dots, 0] \quad (15)$$

This partition is in general $m \times 3$, (one column for each of the three moment directions), and we denote the partial of this partition by the $m \times 3$ matrix

$$\mathbf{d}(L_{xk}) \equiv \frac{\delta \mathbf{G}_k}{\delta L_{xk}} \quad (16)$$

Thus we can simplify Equation (14) as

$$\frac{\delta \ln l}{\delta L_{xk}} = \frac{1}{\sigma^2} \sum_{j=1}^N [\mathbf{d}(L_{xk}) \mathbf{T}_k(j)]^T \mathbf{E}(j) \quad (17)$$

The other two partials for L_{yk} and L_{zk} are similarly formed. This notation now allows us to more compactly describe the 3×1 partials vector with respect to the vector \bar{L}_k , rather than just its individual components L_{xk} , L_{yk} , and L_{zk} :

$$\begin{aligned} \frac{\delta \ln l}{\delta \bar{L}_k} &= \frac{1}{\sigma^2} \sum_{j=1}^N [\mathbf{d}(\bar{L}_k) \mathbf{T}_k(j)]^T \mathbf{E}(j) \\ &= \frac{1}{\sigma^2} \sum_{j=1}^N [\mathbf{I}_3 \otimes \mathbf{T}_k(j)]^T \mathbf{d}(\bar{L}_k)^T \mathbf{E}(j) \end{aligned} \quad (18)$$

where “ \otimes ” denotes the Kronecker product, \mathbf{I}_3 is the 3×3 identity matrix, and $\mathbf{d}(\bar{L}_k)$ is an $m \times 9$ extension of the our definition in (16), $\mathbf{d}(\bar{L}_k) \equiv [\mathbf{d}(L_{xk}), \mathbf{d}(L_{yk}), \mathbf{d}(L_{zk})]$.

If for all p dipoles we define the full $m \times 9p$ partial matrix

$$\mathbf{D} \equiv [\mathbf{d}(\bar{L}_1), \dots, \mathbf{d}(\bar{L}_p)] \quad (20)$$

and the block-diagonal $9p \times 3p$ matrix

$$\mathbf{X}(j) \equiv \begin{bmatrix} \mathbf{I}_3 \otimes \mathbf{T}_1(j) & & 0 \\ & \ddots & \\ 0 & & \mathbf{I}_3 \otimes \mathbf{T}_p(j) \end{bmatrix} \quad (21)$$

we can now compactly write the $3p \times 1$ partials vector with respect to *all* locations \bar{L}_k in θ ,

$$\frac{\delta \ln l}{\delta \theta} = \frac{1}{\sigma^2} \sum_{j=1}^N \mathbf{X}(j)^T \mathbf{D}^T \mathbf{E}(j) \quad (22)$$

This notation allows us to now parallel the work of Stoica [7] in deriving the expectations of the cross products. With the assumption that the noise is zero-mean and white, several of the expectations of the cross products are simply zero. We can group the parameters in ψ as $\psi = [\sigma^2, \mathbf{I}^T, \theta^T]^T$. If we define $\Delta(j) \equiv \mathbf{G}^T \mathbf{D}\mathbf{X}(j)$, $\Delta \equiv [\Delta(1)^T, \dots, \Delta(N)^T]^T$, and $\Gamma \equiv \sum_{j=1}^N (\mathbf{D}\mathbf{X}(j))^T (\mathbf{D}\mathbf{X}(j))$, then the Fisher information matrix partitions nicely into three parts. After taking all expectations, the final result for the Fisher information matrix is

$$\mathbf{J} = \frac{1}{\sigma^2} \begin{bmatrix} \frac{Nm}{2\sigma^2} & 0 & 0 \\ 0 & \mathbf{I}_N \otimes \mathbf{G}^T \mathbf{G} & \Delta \\ 0 & \Delta^T & \Gamma \end{bmatrix} \quad (23)$$

Inversion of this matrix \mathbf{J} gives us the Cramer-Rao lower bound (CRLB) for the error variance. We are particularly interested in the diagonal elements of this inverse, since the CRLB for the i th parameter ψ_i is simply the i -th element of \mathbf{J}^{-1} [8, page 51]. With this partition and using the standard inversion formula [8, page 102], we can express the CRLBs for the variance and the locations as

$$CRLB(\sigma^2) = \frac{2\sigma^4}{Nm} \quad (24)$$

$$\begin{aligned} CRLB(\theta) &= \sigma^2 [\Gamma - \Delta^T [\mathbf{I}_N \otimes (\mathbf{G}^T \mathbf{G})^{-1}] \Delta]^{-1} \\ &= \sigma^2 \left[\sum_{j=1}^N (\mathbf{D}\mathbf{X}(j))^T \mathbf{P}_G^\perp (\mathbf{D}\mathbf{X}(j)) \right]^{-1} \end{aligned} \quad (25)$$

where $\mathbf{P}_G^\perp = (\mathbf{I} - \mathbf{G}\mathbf{G}^T) = (\mathbf{I} - \mathbf{P}_G)$ is the orthogonal complement of the projection matrix for \mathbf{G} , and we use reduced rank forms of \mathbf{G} as necessary to form the pseudoinverse \mathbf{G}^\dagger . For the calculation of the CRLB for the moment time series, if we let $\gamma \equiv CRLB(\theta)/\sigma^2$, then the CRLB for each time j , $j = 1, \dots, N$ is

$$\begin{aligned} CRLB(\mathbf{I}(j)) &= \sigma^2 (\mathbf{G}^T \mathbf{G})^{-1} \\ (\mathbf{I} + \mathbf{G}^T \mathbf{D}\mathbf{X}(j) \gamma \mathbf{X}(j)^T \mathbf{D}^T \mathbf{G} (\mathbf{G}^T \mathbf{G})^{-1}) \end{aligned} \quad (26)$$

4 Computational Results

We conclude by presenting the results of two simulations of MEG data. In the first simulation, data were simulated for the case of three dipoles with fixed location and orientation. Associated with each dipole are three location parameters, three orientation parameters and the associated N -length scalar moment time series. The data were computed for an array of 37 closely spaced sensors radially oriented and positioned on the surface of a sphere of radius 12 cm. A total of 100 time samples were generated and corrupted by additive white Gaussian noise with a SNR of 10dB, where SNR is computed as the ratio of the average magnetic field measurement power to the variance of the noise.

The locations of the three dipoles were estimated using a Nelder-Mead simplex search to effectively maximize the projection of the data onto the subspace spanned by the

matrix \mathbf{G} . The moment time series \mathbf{T} were then found as a linear least-squares fit. The true and estimated locations are listed in Table 1 and the estimated time series are shown in Figure 1 (left), overlaid with the original simulated time series. To approximate a constrained orientation, the identified time series were then fit to a rank one model (per dipole) via an SVD, resulting in the time series displayed in Figure 1 (right). The true and identified moments are displayed in Table 1.

To illustrate the CRLB calculations, in the second simulation we examined the case for one time slice, $N = 1$, and calculated the error variance for the location of one dipole as a function of distance to the array. The dipole was oriented in the x -axis direction and was moved along the z -axis from the coordinate origin out to the array of sensors. The 37 sensors were positioned on the surface of a sphere of radius 12 cm. Figure 2 presents the standard deviation for the error in estimating the xyz coordinates of the dipole. Overlaid on the CRLBs are the results of a 1000 iteration Monte Carlo run for the least-squares estimator. The results show excellent agreement when the dipole is close to the array, but as the dipole nears the coordinate origin, the errors become large, and the Cramer-Rao bound is apparently no longer a tight lower bound.

REFERENCES

- [1] S. J. Williamson, G.-L. Romani, L. Kaufman, and I. Modena, eds., *Biomagnetism: An Interdisciplinary Approach*. New York: Plenum Press, 1983.
- [2] M. Scherg and D. von Cramon, "Two bilateral sources of the late AEP as identified by a spatio-temporal dipole model," *Electroencephalography and clinical Neurophysiology*, vol. 62, pp. 32-44, 1985.
- [3] J. C. Mosher, P. S. Lewis, R. Leahy, and M. Singh, "Multiple dipole modeling of spatio-temporal meg data," *Proceedings of the SPIE*, vol. 1351, July 1990.
- [4] B. Jeffs, R. Leahy, and M. Singh, "An evaluation of methods for neuromagnetic image reconstruction," *IEEE Transactions on Biomedical Engineering*, vol. BME-34, pp. 713-723, September 1987.
- [5] M. Scherg and D. von Cramon, "Evoked dipole source potentials of the human auditory cortex," *Electroencephalography and clinical Neurophysiology*, vol. 65, pp. 344-360, 1986.
- [6] G. H. Golub and V. Pereyra, "The differentiation of pseudo-inverses and nonlinear least squares problems whose variables separate," *SIAM Journal Numerical Analysis*, vol. 10, pp. 413-432, April 1973.
- [7] P. Stoica and A. Nehorai, "MUSIC, maximum likelihood, and Cramer-Rao bound," *IEEE Transactions on Acoustics, Speech and Signal Processing*, vol. 37, pp. 720-741, May 1989.
- [8] J. M. Mendel, *Lessons in Digital Estimation Theory*. Englewood Cliffs, New Jersey 07632: Prentice Hall, Inc., 1987.

Table 1: Estimated Locations and Moments

Table 1. Estimated Locations and Moments									
	Dipole 1			Dipole 2			Dipole 3		
True and Estimated Location (cm)									
	L_x	L_y	L_z	L_x	L_y	L_z	L_x	L_y	L_z
True	2.800	-1.700	8.300	-2.900	-1.600	8.300	0.000	3.300	8.400
Est.	2.798	-1.753	8.236	-2.922	-1.562	8.341	-0.013	3.298	8.490
True and Estimated Moments (from SVD)									
	M_x	M_y	M_z	M_x	M_y	M_z	M_x	M_y	M_z
True	-0.400	0.862	0.311	0.767	0.525	0.369	0.516	-0.797	0.313
Est.	-0.402	0.858	0.319	0.755	0.543	0.366	0.503	-0.805	0.314

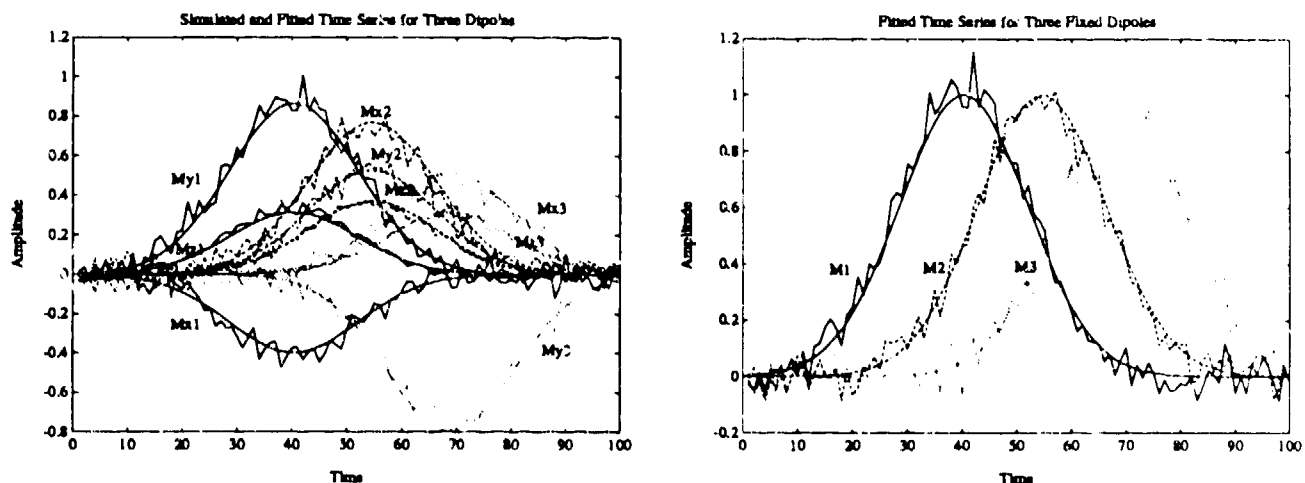


Figure 1: Estimated moment time series for three dipoles. Three dipoles of fixed tangential orientation (no radial component) were given greatly overlapping time series and projected into Cartesian coordinates, one time series per coordinate per dipole. A Nelder-Mead simplex algorithm was used to find the locations. The nine time series were found with a simple least-squares fit, plotted in the left figure. An SVD was then performed on each set of three waveforms to approximate constrained orientations, and the resulting dipole moment magnitude and polarity is plotted in the right figure.

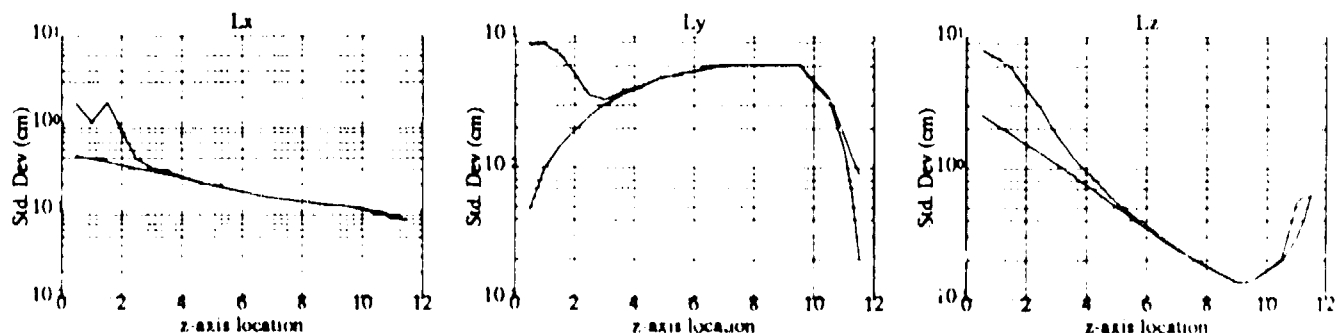


Figure 2: Cramer-Rao lower bounds for a single dipole, overlaid with 1000 iteration Monte Carlo simulations. The dipole was oriented in the x-axis direction and moved along the z-axis until just under the sensor array, which was located at 12 cm on the z-axis. Displayed are the standard deviations in estimating the three coordinate positions of the dipole, as a function of dipole location. The lower curve is the CRLB, the upper one is the Monte Carlo simulations.